International Journal of Antimicrobial Agents A potent HDAC inhibitor blocks Toxoplasma gondii tachyzoite growth and profoundly disrupts parasite gene expression

Thomas Mouveaux, Dante Rotili, Tom Boissavy, Emmanuel Roger, Christine Pierrot, Antonello Mai, Mathieu Gissot

A potent HDAC inhibitor blocks *Toxoplasma gondii* tachyzoite growth and profoundly disrupts parasite gene expression

Thomas Mouveaux[a], Dante Rotili[b], Tom Boissavy[a], Emmanuel Roger[a], Christine Pierrot[a], Antonello Mai[b], Mathieu Gissot[a,*]

[a]Univ. Lille, CNRS, Inserm, CHU Lille, Institut Pasteur de Lille, U1019 - UMR 9017 - CIIL - Center for Infection and Immunity of Lille, F-59000 Lille, France

[b]Dipartimento di Chimica e Tecnologie del Farmaco "Sapienza" Università di Roma, 00185 Rome, Italy

*** Corresponding author:** Univ. Lille, CNRS, Inserm, CHU Lille, Institut Pasteur de Lille, U1019 - UMR 9017 - CIIL - Center for Infection and Immunity of Lille, F-59000 Lille, France. Email : mathieu.gissot@pasteur-lille.fr (Mathieu Gissot)

Abstract

Introduction: Toxoplasmosis is a major health issue worldwide, especially for immune-deficient individuals and the offspring of newly infected mothers. It is caused by a unicellular intracellular parasite called *Toxoplasma gondii*. Although the drugs commonly used to treat toxoplasmosis are efficient, they present serious side effects and adverse events are common. Therefore, there is a need for the discovery of new compounds with potent anti-*Toxoplasma gondii* activity.

Methods: This study tested compounds designed to target enzymes that are involved in the epigenetic regulation of gene expression.

Results: Among the most active compounds, an HDAC inhibitor showing an IC_{50} of 30 nM with a selectivity index above 100 was identified. MC1742 was active at inhibiting the growth of the parasite *in vitro* but also at preventing the consequences of the acute disease *in vivo*. This compound induced hyper-acetylation of histones, while the acetylated tubulin level remained unchanged. After MC1742 treatment, the parasite expression profile was profoundly changed with the activation of genes preferentially expressed in the sexual stages that are normally repressed in the tachyzoite stage.

Conclusions: These findings suggest that this compound disturbs the *Toxoplasma gondii* gene expression program, inducing parasite death.

Keywords: Toxoplasma; Apicomplexa; HDAC; HDAC inhibitors; Malaria; Plasmodium

Introduction

Apicomplexa is a phylum consisting of obligate intracellular protozoan parasites of high transmissibility, which includes various human pathogen species such as *Plasmodium* spp. (causative agent of malaria), *Toxoplasma gondii* (*T. gondii*) (cause of toxoplasmosis) and *Cryptosporidium* spp. (cause of cryptosporidiosis). Although toxoplasmosis is generally asymptomatic in immunocompetent hosts, it can lead to the development of focal central nervous system infections in immunocompromised hosts. *Toxoplasma* is also a clinically important opportunistic pathogen that can cause birth defects or death in the offspring of newly infected mothers and is a threat to immunocompromised individuals. The worldwide seroprevalence of *T. gondii* infection is high and estimated between 30–70% in humans, depending on the geographical areas [1]. The *T. gondii* life cycle is complex, with multiple differentiation and proliferation steps that are key to parasite survival in human and feline hosts [2]. Infection by oocysts containing sporozoites shed by cats or by bradyzoites contaminating meat leads to differentiation into the rapidly growing tachyzoites that are responsible for the clinical manifestations in humans. The tachyzoites are responsible for the acute phase of the disease and their proliferation is the cause of the disease symptoms in intermediate hosts. The latent bradyzoites are thought to persist in the infected host for prolonged periods, due to their ability to evade the immune system and to resist commonly used drug treatments. Bradyzoites also have the ability to reactivate into virulent tachyzoites and cause encephalitis, particularly in immunocompromised hosts [3]. The current treatment for toxoplasmosis consists of the use of pyrimethamine and sulfadiazine. This combination is active against the tachyzoite form of the parasite and therefore the acute phase of the disease. There are currently no drugs that target the latent form of the parasite. Both pyrimethamine and sulfadiazine target the folate pathway, and therefore folinic acid complementation is usually necessary to limit the impact on the patient. This association has long been known to be synergetic for the treatment of toxoplasmosis [4] but the teratogenic effects of pyrimethamine limits its use in pregnant women

[5]. Adverse events are associated with this regimen; > 30% of the patients show adverse events leading to treatment discontinuation, among which bone marrow suppression is one of the most serious side effects [6]. Clindamycin is a second-line drug that can replace sulfadiazine in case of patient allergy, but this antibiotic presents a similar adverse event probability and is less efficient at preventing relapse [7]. Taken together, these observations emphasise the need for a better toxoplasmosis treatment.

To address this need, many compounds have been tested against this parasite [8]. Enzymes mediating epigenetic modifications of histones have rapidly appeared as potential targets, since several compounds designed to inhibit these enzymes can be repurposed [8]. In addition, mechanisms of gene regulation are essential to parasite growth [9,10]. Among the epigenetic modifications of chromatin, histone acetylation has undoubtedly been the most pre-eminent target to be tested against *T. gondii* [11] and other parasites [12]. Few compounds potentially inhibiting histone acetyltransferases (HATs) [13,14] and deacetylases (HDACs) [15–19] have been shown to be active against *T. gondii*, indicating that histone acetylation is crucial for tachyzoite survival and therefore a promising therapeutic target. Moreover, most *T. gondii* HAT and HDAC enzymes are essential for in vitro growth of tachyzoites [20].

This study investigated the anti-*T. gondii* activity of compounds that target epigenetic mechanisms and have been shown to be active against *Plasmodium falciparum* (*P. falciparum*) [21]. It was demonstrated that a known HDAC inhibitor showed potent activity against the tachyzoite form of this parasite both in vitro and in a mouse model of infection. MC1742 presented a lower IC_{50} than pyrimethamine and other hydroxamate-based HDAC inhibitors. Treatment with MC1742 strongly increased the level of parasite histone acetylation and profoundly affected gene expression, suggesting a crucial role for histone deacetylation in maintaining the tachyzoite-specific gene expression program.

Material and Methods

Parasite strains and culture

Toxoplasma gondii tachyzoites of the RH, 76K, PTG-LUC-GFP, RH-LUC GFP strains and the two strains bearing the mutated residues T99A and T99I of TgHDAC3 [17] (a gift from Dr Hakimi) were propagated in vitro in human foreskin fibroblasts (HFF, acquired from the American Type Culture Collection) using Dulbecco's Modified Eagle Medium supplemented with 10% foetal calf serum, 2 mM glutamine and 1% penicillin-streptomycin. Tachyzoites were grown in ventilated tissue culture flasks at 37 °C and 5% CO_2.

Intracellular growth assays

For intracellular treatment with the compounds, 8 x 10^4 parasites, at a multiplicity of infection of ca. 2, were inoculated on HFF cells. Parasites were left to invade for 4 hours; the media were then changed and replaced with media containing either Dimethylsulfoxide (DMSO) or a chemical compound to be tested. After 24 hours, the coverslips were then fixated using 4% paraformaldehyde (PFA). The parasite nuclei were stained with anti-TgEno2 (provided by S. Tomavo) and the parasites per vacuole were counted. Quantification of immunofluorescence assays was carried out manually by counting the concerned signal by visual observation. Signal corresponding to 100 vacuoles was counted for each replicate. Three independent experiments were performed.

For extracellular treatment, 8 x 10^4 parasites were treated for 4 hours with either DMSO or a chemical compound to be tested. The media were then changed and the 8 x 10^4 parasites were deposited onto HFF cells in a well of a 24-well plate for each condition. After 24 hours, the coverslips were then fixated using 4% PFA and processed as above.

Plaque assay

Two hundred parasites were inoculated on HFF cells grown in a six-well plate for 7 days in normal media and media supplemented with the compounds or DMSO. Host cells were fixated with methanol and then stained using a Crystal Violet solution. Three independent experiments were performed.

***Dolichos biflorus* lectin labelling**

Type II parasites of the 76K strain (8 x 10^4 parasites) were inoculated on HFF cells. Parasites were left to invade for 4 hours; the media were then changed and replaced with media containing either DMSO or MC1742 (0.5 µM). After 24 hours, the coverslips were then fixated using 4% PFA and stained using *Dolichos biflorus* lectin (FITC, Vector Laboratories). Quantification of immunofluorescence assays was carried out manually by counting the concerned signal by visual observation. Signal corresponding to 100 vacuoles was counted for each replicate. Three independent experiments were performed.

RNA sample collection and library preparation

RNA samples were collected after infecting HFF cells with the RH strain for 24 hours and then treated for 6 hours with either DMSO or MC1742 (0.5 µM). Parasites were extracted and purified from the host cell before being lysed in Trizol. RNA was extracted as per manufacturer's instruction and genomic DNA was removed using the an RNase-free DNase I Amplification Grade Kit (Sigma). All RNA samples were assessed for quality using an Agilent 2100 Bioanalyzer. RNA samples with an integrity score ≥ 8 were included in the RNA library preparation. Triplicates (biological replicates) were produced for each condition. The TruSeq Stranded mRNA Sample Preparation kit (Illumina) was used to prepare the RNA libraries

according to the manufacturer's protocol. Library validation was carried out using DNA high-sensitivity chips passed on an Agilent 2100 Bioanalyzer. Library quantification was carried out by quantitative PCR.

RNA-seq and analysis

Clusters were generated on a flow cell with a cBot using the Cluster Generation Kit (Illumina). Libraries were sequenced as 50 bp-reads on a HiSeq 2500 using the sequence by synthesis technique (Illumina). HiSeq control software and a real-time analysis component were used for image analysis. Illumina's conversion software (bcl2fastq 2.17) was used for demultiplexing. Datasets were aligned with HiSAT2 v2.1.0 [22] against the *T. gondii* ME49 genome from (ToxoDB-39) [23]. Expression for annotated genes was quantified using htseq-count and differential expression measured by DESeq2. *P*-values for multiple testing were adjusted using the Benjamini-Hochberg method. Differentially expressed genes with an adjusted *P*-value < 0.05 and log2 fold-change $> 1 < -1$ were considered in this study. RNA-seq data that supported the findings of this study have been deposited in the GEO database under the accession number GSE175919.

Quantitative real time PCR (RT-qPCR)

Primers used in the RT-qPCR experiments are the following: SRS48K (TGME49_207010; forward: GATGTGCATGTGTGCTACTA; reverse: GTTTGGGCACTCCTTTGA), Gra11b (TGME49_237800; forward: AAACTGACGCAGGAAGTG; reverse: ATCCGGTGGTCGGATTAT) and TGME49_277060 (forward: CGTTCTGTTCTCCTGACTATG; reverse: CCTGAACCTCTTCACCTTTC). Tachyzoite RNA was isolated using Trizol Reagent, according to manufacturer's protocol, and purified after an RNase-free DNase I Amplification grade treatment. An Agilent 2100 Bioanalyzer was

used to assess the integrity of the RNA samples that were then quantified with a NanoVue Plus Spectrophotometer. Total cDNA was generated using the Maxima Reverse Transcriptase kit with 1 µg of total RNA and oligo (dT) in a final volume of 20 µL, as recommended by the manufacturer. RT-qPCR was performed using the SYBR® Selected Master Mix, according to manufacturer's instructions, using 3 µM of each primer and ca. 10 ng of cDNA in nuclease-free water to a final volume of 20 µL. Change in expression of individual genes was represented by relative fold change in the Cq values as ΔΔCq (*TgTub* served as reference gene).

ChIP-qPCR

Intracellular parasites of the 76K strain were grown for 24 hours and then treated for 24 hours with 0.5 µM of MC1742 or DMSO. ChIP was performed as previously described [24] using the anti-H4ac antibody (#06-866; Millipore). The input samples were eluted in 30 µL, while the IP samples were eluted in 10 µL. Primers used in the ChIP-qPCR experiments are the following: SRS48K promoter (TGME49_207010; forward: CGGAGACCAGCATTTGATTT; reverse: AATGGCTTTGCCTTTGTTTG), Gra11b promoter (TGME49_237800; forward: TCCGACAGGGATCTGTTTTC; reverse: TGACTTTGTCAACGCACCTC), TGME49_277060 promoter (forward: CCTTTGCATGTGACCCCTAT; reverse: GATGGCGAAGGATTTGATGT) and ROP16 promoter (forward: CCGTCAGTGGTAGGCCTTTT; reverse: TTGGTACGGATCTGCCCAAC). ChIP-qPCR was performed using the SYBR Selected Master Mix, according to manufacturer's instructions, using 3 µM of each primer, 1 µL of input and IP DNA to a final volume of 20 µL. Change in the level of H4ac for individual promoter is represented by relative fold change in the Cq values as ΔΔCq (input served as reference) comparing MC1742 and DMSO treated samples.

IC_{50} calculation

To measure the IC_{50} of each compound, a luminometric assay was performed on a parasitic strain expressing luciferase. Each well of the 96-well plates was infected with 25.10^3 parasites. For each compound, 10 concentrations from 2 µM to 1 nM were tested. Each condition was carried out in triplicate. After 24 hours of growth for the type I strain or 40 hours for the type II strain, the plate was washed twice with PBS and 50 µL of lysis buffer (Glo Lysis Buffer, Promega) was added in each well. The plates were then frozen at –80 ° C for at least an hour. The quantity of parasite was measured by detecting the emission of light after the addition of the luciferase substrate (Luciferase Assay System, Promega) using a SPARK plate reader (TECAN). After thawing the plate, 50 µL of luciferase substrate was automatically injected into each well and then the quantity of light was read for 1 second. The measured values were used to plot a regression curve and calculate the IC_{50} using Graphpad Prism.

Mice infections

Animal housing and experimentation were carried out in accordance with the French Council in Animal Care guidelines for the care and use of animals and following the protocols approved by the Institut Pasteur de Lille's ethical committee (number #11082-2017072816548341 v2). Prior to mice infection, intracellular parasites were purified by sequential syringe passage with 17-gauge and 26-gauge needles and filtration through a 3-µm polycarbonate membrane filter. For studying the acute phase of toxoplasmosis, 6–8-week-old Balb/c mice were infected intraperitoneally using 10^5 parasites of the 76K strain. One day after infection, the mice were intraperitoneally treated with a dose of MC1742 at a concentration of 10 mg/kg (resuspended in 7% DMSO) or the solvent only (7% DMSO) daily for 7 days. Survival of mice was followed until all apparent signs of disease disappeared. For studying the latent phase of infection, 6–8-

week-old Balb/c mice were intraperitoneally infected using 10^2 parasites of the 76K strain. When studying the effect of the treatment on cyst establishment, the mice were intraperitoneally treated with either DMSO or MC1742 at a dose of 10 mg/kg daily for 7 days, 24 hours after infection. The mice were then left untreated for 4 weeks before being euthanised. When studying the effect of the treatment on the established cysts, the mice were intraperitoneally treated with either DMSO or MC1742 at a dose of 10 mg/kg daily for 7 days, 4 weeks after infection. The mice were then euthanised and their brains were collected and homogenised individually. Cysts were counted after *Dolichol biflorus* lectin (DBA-FITC, Vector Laboratories) labelling of the cyst wall for 30 minutes at room temperature to a dilution of 1:400 in PBS. One-fifth of the brain of each mouse was scored for the presence of lectin-positive cysts.

Western blot

Intracellular parasites were grown for 24 hours and then treated overnight with 0.5 µM of MC1742 or DMSO. Parasites were then purified from the host cell by sequential syringe passage with 17-gauge and 26-gauge needles and filtration through a 3-µm polycarbonate membrane filter. This enabled collection of parasites that were free from the host-cell material. Parasites were resuspended in 1X Laemmli buffer to prepare the total protein extracts. The protein samples were then fractionated on a 15% SDS-polyacrylamide electrophoresis gel and then transferred onto a nitrocellulose membrane. The antibodies used were: anti-acetylated Histone H4K8 (ab15823; 1:1000); anti-acetylated Histone H3K9 (ab4441; 1:1000); anti-Histone H3 targeted at the C-terminus (07-690 EMD; 1:5000); anti-tri-methylated Histone H3K4 (ab8580; 1:1000); anti-acetylated tubulin (T7451; 1:10000); and anti-alpha tubulin (GTX628802; 1:1000). Chemiluminescent detection of bands was carried out using Super Signal West Femto Maximum Sensitivity Substrate.

Statistics and Reproducibility

All data were analysed with GraphPad Prism software version 8 (San Diego, California, USA). Differences in the means were assessed by Student's *t* test. Differences in survival curves were assessed by a Log-rank (Mantel-Cox) test. In all cases, *P*-values were two-sided and $P < 0.05$ was considered as significant. All experiments were repeated at least three times using biologically independent replicates.

Results

Compounds potentially active against epigenetic enzymes inhibited tachyzoite growth

The anti-*T. gondii* activity of four compounds that potentially targeted enzymes involved in chromatin modification was tested (Table 1). Two compounds had potential anti-HDAC activity (MC1742 and Mocetinostat) and two compounds were potentially targeted at DNA methylation (MC3681 and MC3973).

To test the anti-*T. gondii* activity of these compounds, their ability to inhibit the parasite proliferation in vitro was first investigated. The parasites were treated while intracellular with three different concentrations of compounds (Figure 1A). The parasites were left to invade the host cells for 4 hours and then treated with the compounds at different concentrations during 24 hours. The number of parasites per vacuole was then recorded as a measurement of their ability to grow intracellularly in the presence of the compounds. In the presence of DMSO (solvent used to dissolve the compounds), the parasites were able to grow to a mean of nine parasites per vacuole. Pyrimethamine was used as a positive control, which was able to ablate most of the intracellular growth (mean parasite per vacuole: 1.34). All the tested compounds showed a similar inhibitory effect at 10 µM. However, MC1742 was able to inhibit the parasite growth at a concentration of 1 µM (Figure 1A), indicating that this compound may be as efficient as the reference pyrimethamine treatment to inhibit intracellular growth.

The action of these compounds to inhibit the parasite in its extracellular form was also investigated. To this end, the extracellular parasites were treated with different compound concentrations for 4 hours, which were washed away and these parasites were left to grow for 24 hours (Figure 1B). The number of parasites per vacuole was recorded as a measurement of the compound activity. As expected, DMSO and pyrimethamine led to a mean growth of five parasites per vacuole. Indeed, pyrimethamine is a known inhibitor of intracellular growth and is not active when the parasites are treated extracellularly [25]. Treating the parasites in their

extracellular form did not significantly affect their ability to grow inside the cell, with the exception of MC3973; this compound potentially targeting DNA methyl-transferases showed an effect at a concentration of 1 μM (Figure 1B).

To investigate the ability of these parasites to grow in the presence of the inhibitors during a 7-day period, a plaque assay was performed that measured the ability of the parasite to grow and invade the host cells for several cycles (Figures 1C and 1D). The percentage of the lysed surface on each well of the plaque assay was determined to assess the inhibitory activity of these compounds. In this experiment, pyrimethamine and MC1742 were able to totally abrogate the presence of plaques (Figure 1C). Most of the compounds were active at 1 μM but had little to no effect at lower concentrations, except for MC1742, which was still active at 0.1 μM (Figure 1D).

Compounds potentially active against epigenetic enzymes presented an IC_{50} ranging from the micromolar to the nanomolar

To precisely measure the IC_{50} of these compounds, a new assay was designed using luciferase expressing parasites. This assay was performed in 96-well plates using bioluminescent type I or type II parasites [26]. The IC_{50} of the compounds was quantified and it was found that MC1742 was able to inhibit the growth of tachyzoites at a much lower concentration than the other compounds (Table 2). Of note, the calculated IC_{50} was similar for both type I and type II parasites, indicating that the inhibitory effect was comparable irrespective of the parasite strain used (Table 2). The selectivity index (SI) of some of these compounds was also calculated and it was found that MC1742 presented an SI > 100, while other compounds showed an SI < 10. Overall, MC1742 was the most efficient compound on tachyzoite growth and presented an attractive selectivity index (Table 2).

The inhibitory activity of MC1742 was compared with pyrimethamine and other known HDAC inhibitors. Trichostatin A, suberoylanilide hydroxamic acid (SAHA) and Scriptaid are hydromate-based HDAC inhibitors, while Apicidin is a tetracyclic peptide HDAC inhibitor known to inhibit *T. gondii* growth [15]. The IC_{50} of these drugs was measured in parallel (Table 3). Other HDAC inhibitor compounds that presented a similar chemical structure to MC1742 were also included in the assay (MC1714, MC1745 and MC2026; Table 3). Overall, MC1742 was the most effective compound and presented IC_{50} values that were 10 times smaller than pyrimethamine (Table 3).

MC1742 was effective at preventing acute disease but failed to reduce the cyst burden

Having demonstrated that MC1742 was a very potent inhibitor of parasite growth in vitro, its ability to prevent the outcome of the acute disease was assessed in a mouse model. Balb/c mice were infected with a lethal dose of type II strain. The survival of mice was recorded for 15 days (Figure 2A). Mice were treated daily for 7 days with a dose of 10 mg/kg of MC1742 or DMSO for the control group. Whilst the survival rate of the control group was 6% (n = 32), > 80% (n = 32) of the mice survived in the treated group, indicating that MC1742 was efficient at preventing the outcome of acute disease in this mouse model (Figure 2A).

To test the effect of the molecule on the established chronic form of the parasite, mice were injected with a sub-lethal dose of type II parasites and left untreated for 4 weeks. They were subsequently treated daily for 7 days with a dose of 10 mg/kg of MC1742 or vehicle (DMSO) as control. The mice brains were then collected and the number of cysts per brain was measured (Figure 2B). The recorded cyst numbers were similar in both MC1742-treated and DMSO-treated mice, indicating that MC1742 failed to reduce the established cyst burden with this regimen (Figure 2B).

To test the effect of the molecule on the establishment of the chronic form of the parasite, mice were injected with a sub-lethal dose of type II parasites and subsequently treated daily for 7 days with a dose of 10 mg/kg of MC1742 or vehicle (DMSO) as control. The mice brains were then collected and the number of cysts per brain was measured (Figure 2C). The recorded cyst numbers were smaller in the MC1742-treated mice when compared with the control group, indicating that MC1742 treatment reduced the establishment of cysts, probably by reducing the number of tachyzoites at the beginning of infection (Figure 2C).

MC1742 was a potent inhibitor of the parasite HDACs

MC1742 is known to inhibit human HDACs of class I/IIb [27]. To assess the ability of MC1742 in inhibiting the *T. gondii* HDACs, the relative level of acetylation of several parasite histones was assessed. The parasite was treated with MC1742 or DMSO and specific antibodies were used to measure the relative level of acetylation of Histone H4 at the lysine 8 position (H4K8ac, Figure 3A) and Histone H3 at the lysine 9 position (H3K9ac, Figure 3B). As control, it was verified that the level of the Histone H3 (Figure 3C) and the level of methylation of Histone H3 at the lysine 4 position (H3K4me3) were unchanged (Figure 3D). These experiments showed that the level of histone acetylation was strongly enhanced in the presence of MC1742, while the level of H3K4me3 was unchanged (Figure 3E). Whether the acetylation level of non-histone proteins was affected by the MC1742 treatment was also verified. For that purpose, the level of acetylation of α-tubulin at the lysine 40 position was measured by western blot after MC1742 treatment (Figure 3F) and showed that there were no significant changes between the DMSO and MC1742 treatment (Figure 3G). This showed that MC1742 inhibits the parasite HDACs that specifically deacetylate histones.

MC1742 profoundly perturbed the tachyzoite expression program

To determine how MC1742 might influence parasite gene expression, the changes in the tachyzoite transcriptome after MC1742 treatment were measured using RNA-seq. Parasites were left to grow during 24 hours and then treated with either DMSO or MC1742 for 6 hours. A *P*-value cut-off of 0.05 and a minimum two-fold change were used to identify differentially expressed genes (DEGs) using the DESEQ2 program. The differential gene expression was represented using a volcano plot (Figure 4A), which clearly shows that the majority of DEGs are upregulated transcripts after 6 hours of MC1742 treatment. Indeed, 1671 genes were found to be upregulated, while 592 were found to be downregulated. The expression of three transcripts that were upregulated in the presence of MC1742 was verified using RT-qPCR and the results were confirmed by RNA-seq (Figure 4B). Relative enrichment of acetylated Histone 4 at the promoter of genes that were upregulated after MC1742 treatment (SRS48K, Gra11b, TGME49_277060) and a control locus (ROP16 promoter) with unchanged expression after MC1742 treatment were also verified (Figure 3C). A ration of the relative H4ac enrichment when compared with the samples treated by MC1742 and DMSO was produced. This data revealed the presence of up to six times more H4ac enrichment at the promoter of the selected genes than identified as upregulated (Figure 4C). To better assess the nature of the upregulated or downregulated genes, a heat-map representing the expression of each individual gene expression during the life cycle of *T. gondii* based on previously published results was produced [28]. It was first observed that the downregulated genes were mainly expressed during the tachyzoite stage (Figure 4D). In contrast, the upregulated genes were preferentially expressed during the sexual cycle in the definitive host and to a lesser extent at the bradyzoite stage (Figure 4E). These data indicate that MC1742 treatment induces the expression of genes that are normally not expressed at the tachyzoite stage. These genes are preferentially expressed during the sexual cycle, as exemplified by Gra11b (Figure 4B).

MC1742 induced expression profile changes that closely reassembled those induced by TgHDAC3 inhibition

The expression profiling performed using RNA-seq highlighted the particular expression profile induced after the treatment of tachyzoites with MC1742. This expression profile was compared with previously published data that reported the transcriptome changes of tachyzoites in a TgMORC mutant [29] or after treatment of the parasite with the TgHDAC3-specific inhibitor FR235222 [17]. TgMORC closely associates with TgHDAC3 and enables its binding to DNA [29]. The expression profile of the TgMORC mutant was first compared with the one induced by MC1742 treatment (Figure 5A). It showed that > 80% of the genes upregulated after MC1742 treatment overlap with the genes upregulated in the TgMORC mutant (Figure 5A). In contrast, < 1% of the genes downregulated after MC1742 treatment overlap with the genes upregulated in the TgMORC mutant (Figure 5A). The list of upregulated genes in the absence of TgMORC was then compared with the one induced by MC1742 treatment or by the TgHDAC3-specific inhibitor FR235222 (Figure 5B). Similar results were found with an overlap of > 70% between the expression profile induced by MC1742 treatment or by the TgHDAC3-specific inhibitor FR235222 (Figure 5B). These data underline that both inhibitors and the absence of MORC produce a very similar expression profile that may be partly due to the inhibition of TgHDAC3. To further investigate TgHDAC3 as a potential target for MC1742, this compound was tested on two mutant strains bearing a mutation on TgHDAC3 that increases the strain resistance to the TgHDAC3-specific inhibitor FR235222 [17] (Figure 5C). When comparing the growth ability at different concentrations (from 100 mM to 750 µM), no significant difference in growth was identified, indicating that these mutations are insufficient to confer resistance to MC1742.

It was also checked whether MC1742 was able to induce tachyzoite to bradyzoite differentiation, by measuring the percentage of the *Dolichos biflorus* lectin labelled vacuole

after 24 hours of MC1742 treatment (Figure 5D). The TgHDAC3-specific inhibitor FR235222 was shown to induce differentiation [17]. The treatment of tachyzoites of a type II strain with MC1742 did not induced differentiation (Figure 5D), suggesting that different mechanisms are at play during the inhibition of growth by these two compounds.

Discussion

This study explored the anti-*T. gondii* activity of compounds targeting epigenetic mechanisms. Gene regulation is crucial for controlling the establishment of expression profiles and adapting to changing environments during the life cycle of the parasite [10]. Numerous enzymes that can modify or remodel chromatin have been identified in the *T. gondii* genome [30]. Their putative essential role during the parasite life cycle and the possibility of drug repurposing designate them as attractive drug targets. Inhibiting these enzymes to abrogate parasite proliferation has been employed in *T. gondii* and other apicomplexan parasites [21]. The current study tested compounds potentially targeting a variety of enzymes (Table 1). Surprisingly, MC3681 and MC3973, two compounds targeting DNA methyl-transferases, were able to prevent parasite growth, although at a high concentration (10 µM). *T. gondii* has been shown to lack detectable DNA methylation at the tachyzoite stage [31]. Therefore, it is most likely that this inhibitor at this high concentration may target other enzymatic activities, such as RNA methylation, that have been shown to be essential for parasite survival [32,33]. The cytotoxic effect on host cells at 10 µM (Table 2) may also explain the results presented in Figure 1 for these two compounds. MC3681 has been shown to be active against *P. falciparum* and *Plasmodium berghei* at much lower concentrations [21], in line with the biological relevance of DNA methylation in these parasites [34]. Therefore, DNA methylation should not be regarded as an important target in *T.* gondii, in contrast to other apicomplexan parasites such as *P. falciparum.*

MC1742 was the most effective compound tested in this study. It was effective at inhibiting growth in vitro, showing an IC_{50} that was lower than pyrimethamine and other hydroxamate-based compounds. However, Apicidin, a tetracyclic peptide HDAC inhibitor, showed a better IC_{50} than MC1742 in vitro. Hydroxamate-based compounds have been investigated as potential HDAC inhibitors in parasites [12]; they are potent inhibitors of the parasite enzymes and present attractive selectivity indexes [12]. MC1742 is another example of the importance of the enzymatic activities carried out by HDACs for the survival of apicomplexan parasites in vitro. Further research to improve the MC1742 compound may focus on increasing its anti-*T. gondii* activity and bioavailability. MC1742 was also effective at preventing the outcome of the acute disease. Surprisingly, MC1742 showed an IC_{50} in the low nanomolar range against *P. falciparum* but was unable to inhibit the growth of the parasite in vivo [21], whichever the administration route (intravenous or by oral gavage) employed; this might have been due to the bioavailability of the compound in the blood. However, pharmacokinetics studies revealed that MC1742 concentration in the serum of mice was as high as 10 μM, 30 minutes after intra-venous injection with 50 mg/kg of the compound [21]. In contrast, MC1742 has a strong activity in vitro and in vivo to prevent the outcome of acute toxoplasmosis. Treating the mice during the acute phase also reduced the brain cyst burden; however, it was most likely due to the activity of the compound against tachyzoites. MC1742 was not active against the parasite on established cysts; this may be due to the low penetration/availability and accumulation/concentration of the molecule in the brain where bradyzoite cysts reside. Indeed, the blood-brain barrier could filter away the compound. Alternatively, the cyst wall may be impermeable enough to shield the bradyzoites from the compound. Also, the compound may not be active against the bradyzoite stage that divides at a slower pace than tachyzoites. There are currently no drugs available to treat established bradyzoite infection and only a few compounds have been shown to reduce the cyst burden

[35,36]. There is a need to develop new in vitro systems that would enable the testing of compounds against bradyzoites. Organoids or primary brain or muscle cell in vitro culture may open this new research avenue [37].

This study investigated the molecular pathways that were targeted by the MC1742 inhibitor. It showed that Histone de-acetylation is the primary target of the compound, with little to no effect on tubulin acetylation or histone methylation. This is in line with the expression profile that was found to be profoundly changed after a 6-hour treatment with MC1742, as measured by RNA-seq. In good concordance with the increased level of acetylation of histones in the treated parasites, a dramatic increase in expression of transcripts that are not expressed in normal conditions in tachyzoites (up-regulation in the treated group) was observed. In particular, the upregulation of number of genes whose expression is normally restricted to the sexual stages that occur in the feline host (definitive host) was observed. A good example is the *TgGRA11b* transcript, whose expression is normally restricted to merozoites [38]. The current study also verified the level enrichment of acetylated histones at the promoter of selected transcripts. An increased level of histone acetylation at the promoter of the genes that were upregulated after 1742 treatment was reported. This indicates that the repression of gene expression in tachyzoites is directly under control of the acetylation level of histones. Therefore, an increased level of histone acetylation is sufficient to promote the expression of genes that are normally repressed at this stage. Of note, the level of histone methylation seemed to be unchanged by MC1742 treatment as measured by western blot. This indicates that there might be a limited interplay between the global level of histone acetylation and the global level of histone methylation, even though both H3K9ac and H3K4me3 are present at active promoters in tachyzoites [24]. In summary, inhibition of the parasite HDAC indicates that the level of histone acetylation may be the major determinant for the activation or repression of gene expression in *T. gondii* tachyzoites.

Cell cycle defects were recently shown to occur in *T. gondii* tachyzoites treated with hydroxamate-based compounds [19]. The current study observed a drastic effect on the growth of parasites treated by MC1742. In particular, these parasites were unable to proceed with the normal cell cycle, since vacuoles with one parasite were pre-eminent after 24 hours of treatment. This indicates that similar cell cycle defects probably occur in MC1742-treated parasites. It was noticed that Cdk-related kinases (TgCrk2-L1 and TgCrk5-L1) [39], that are normally specifically expressed in merozoites, were overexpressed after MC1742 treatment. Notably, the expression of these kinases may be sufficient to induce cell cycle defects. However, it is difficult to pinpoint the effect of individual genes when > 1000 transcripts are expressed at a stage they should not be.

Toxoplasmosis gondii encodes five potential HDACs (TgHDAC1–5), which are expressed at the tachyzoite stage [11] and could in principle be targeted by MC1742. This compound is described as human class I/IIb HDAC inhibitor [27] and therefore could inhibit the activity of any of these enzymes. To try to learn more about the potential target of MC1742, the current study compared RNA-seq results that were obtained by a specific TgHDAC3 inhibitor (FR235222) [17] or by inhibiting the binding of TgHDAC3 to chromatin (TgMORC mutant) [29]. The high overlap of the expression profile, with > 70% or 80%, respectively, between these two datasets and the RNA-seq results presented here suggests that the potential target of MC1742 may also be TgHDAC3. However, it cannot be excluded that the activity of other HDACs was affected by the compound. The generation of a strain resistant to MC1742 might have been a way to confirm this hypothesis. Unfortunately, such a mutant strain was unable to be produced after several attempts (data not shown). To better assess TgHDAC3 as a potential target of MC1742, the effect of the compound was tested on two strains that carry a mutation of TgHDAC3 that elicits resistance to the FR235222 compound [17]; however, these strains exhibited comparable growth at different concentrations of MC1742. This may indicate

that the resistance mechanism is different for the two compounds. The different structure of the compounds cyclopeptide FR235222 and hydroxamate-based MC1742 may also explain why the induced mutation did not confer increased resistance to MC1742. Therefore, this experiment did not draw definitive conclusion on the identity of the MC1742 targets. Since MC1742 does not induce the expression of TgCST1 (as measured by DBA labelling), this suggests that this compound has different mechanisms of action to FR235222, which was shown to strongly induce differentiation. However, MC1742 treatment results in very comparable dysregulation of gene expression to FR235222 at the tachyzoite stage.

In conclusion, this study identified an HDAC inhibitor that shows a potent anti-*T. gondii* activity in vitro and in vivo in a mouse model of the acute disease. MC1742 treatment profoundly perturbed the normal tachyzoite expression profile and potentially targeted the activity of TgHDAC3 and other HDACs. Overall, MC1742 is a promising compound for future treatment of the acute phase of toxoplasmosis.

Acknowledgments

The authors wish to thank Dr Jamal Khalife for critically reading the manuscript and Dr Hakimi for providing the TgHDAC3 mutant strains. This work was supported by Centre National de la Recherche Scientifique (CNRS), Institut National de la Santé et de la Recherche Médicale (inserm) and the Région Haut de France.

Declarations

Funding: No funding.

Competing Interests: None.

Ethical Approval: Not required.

References

1. Montoya JG, Liesenfeld O. Toxoplasmosis. *Lancet Lond Engl* 2004;**363**:1965–76.

2. Kim K, Weiss LM. Toxoplasma gondii: the model apicomplexan. *Int J Parasitol* 2004;**34**: 423–32.

3. Munoz M, Liesenfeld O, Heimesaat MM. Immunology of Toxoplasma gondii. *Immunol Rev* 2011;**240**:269–85.

4. Eyles DE, Coleman N. An evaluation of the curative effects of pyrimethamine and sulfadiazine, alone and in combination, on experimental mouse toxoplasmosis. *Antibiot Chemother Northfield Ill* 1955;**5**:529–39.

5. Hickl EJ, Mohr U, Martius G. [Animal experimental studies on the problem of fetal damage by pyrimethamine]. *Arch Gynakol* 1964;**199**:634–40.

6. Ben-Harari RR, Goodwin E, Casoy J. Adverse Event Profile of Pyrimethamine-Based Therapy in Toxoplasmosis: A Systematic Review. *Drugs RD* 2017;**17**:523–44.

7. Katlama C, De Wit S, O'Doherty E, Van Glabeke M, Clumeck N. Pyrimethamine-clindamycin vs. pyrimethamine-sulfadiazine as acute and long-term therapy for toxoplasmic encephalitis in patients with AIDS. *Clin Infect Dis Off Publ Infect Dis Soc Am* 1996;**22**:268–75.

8. Alday PH, Doggett JS. Drugs in development for toxoplasmosis: advances, challenges, and current status. *Drug Des Devel Ther* 2017;**11**:273–93.

9. Gissot M, Kim K, Schaap D, Ajioka JW. New eukaryotic systematics: a phylogenetic perspective of developmental gene expression in the Apicomplexa. *Int J Parasitol* 2009;**39**:145–51.

10. Gissot M, Kim K. How epigenomics contributes to the understanding of gene regulation in Toxoplasma gondii. *J Eukaryot Microbiol* 2008;**55**:476–80.

11. Vanagas L, Jeffers V, Bogado SS, Dalmasso MC, Sullivan WJ, Angel SO. Toxoplasma histone acetylation remodelers as novel drug targets. *Expert Rev Anti Infect Ther* 2012;**10**:1189–201.

12. Fioravanti R, Mautone N, Rovere A, Rotili D, Mai A. Targeting histone acetylation/deacetylation in parasites: an update (2017-2020). *Curr Opin Chem Biol* 2020;**57**:65–74.

13. Smith AT, Livingston MR, Mai A, Filetici P, Queener SF, Sullivan WJ. Quinoline derivative MC1626, a putative GCN5 histone acetyltransferase (HAT) inhibitor, exhibits HAT-independent activity against Toxoplasma gondii. *Antimicrob Agents Chemother* 2007;**51**:1109–11.

14. Jeffers V, Gao H, Checkley LA, Liu Y, Ferdig MT, Sullivan WJ. Garcinol Inhibits GCN5-Mediated Lysine Acetyltransferase Activity and Prevents Replication of the Parasite Toxoplasma gondii. *Antimicrob Agents Chemother* 2016;**60**:2164–70.

15. Darkin-Rattray SJ, Gurnett AM, Myers RW, Dulski PM, Crumley TM, Allocco JJ, et al. Apicidin: a novel antiprotozoal agent that inhibits parasite histone deacetylase. *Proc Natl Acad Sci USA* 1996;**93**:13143–7.

16. Strobl JS, Cassell M, Mitchell SM, Reilly CM, Lindsay DS. Scriptaid and suberoylanilide hydroxamic acid are histone deacetylase inhibitors with potent anti-Toxoplasma gondii activity in vitro. *J Parasitol* 2007;**93**:694–700.

17. Bougdour A, Maubon D, Baldacci P, Ortet P, Bastien O, Bouillon A, et al. Drug inhibition of HDAC3 and epigenetic control of differentiation in Apicomplexa parasites. *J Exp Med* 2009;**206**:953–66.

18. Loeuillet C, Touquet B, Oury B, Eddaikra N, Pons JL, Guichou JF, et al. Synthesis of aminophenylhydroxamate and aminobenzylhydroxamate derivatives and in vitro screening for antiparasitic and histone deacetylase inhibitory activity. *Int J Parasitol Drugs Drug Resist* 2018;**8**:59–66.

19. Araujo-Silva CA, De Souza W, Martins-Duarte ES, Vommaro RC. HDAC inhibitors Tubastatin A and SAHA affect parasite cell division and are potential anti-Toxoplasma gondii chemotherapeutics. *Int J Parasitol Drugs Drug Resist* 2020;**15**: 25–35.

20. Sidik SM, Huet D, Ganesan SM, Huynh M-H, Wang T, Nasamu AS, et al. A Genome-wide CRISPR Screen in Toxoplasma Identifies Essential Apicomplexan Genes. *Cell* 2016;**166**:1423–35.e12.

21. Bouchut A, Rotili D, Pierrot C, Valente S, Lafitte S, Schultz J, et al. Identification of novel quinazoline derivatives as potent antiplasmodial agents. *Eur J Med Chem* 2019;**161**:277–91.

22. Kim D, Paggi JM, Park C, Bennett C, Salzberg SL. Graph-based genome alignment and genotyping with HISAT2 and HISAT-genotype. *Nat Biotechnol* 2019;**37**:907–15.

23. Gajria B, Bahl A, Brestelli J, Dommer J, Fischer S, Gao X, et al. ToxoDB: an integrated Toxoplasma gondii database resource. *Nucleic Acids Res* 2008;**36**:D553-556.

24. Gissot M, Kelly KA, Ajioka JW, Greally JM, Kim K. (2007) Epigenomic Modifications Predict Active Promoters and Gene Structure in Toxoplasma gondii. *PLoS Pathog* 2007;**3**:e77.

25. Reynolds MG, Oh J, Roos DS. In Vitro Generation of Novel Pyrimethamine Resistance Mutations in the Toxoplasma gondii Dihydrofolate Reductase. *Antimicrob Agents Chemother* 2001;**45**:1271–7.

26. Saeij JPJ, Boyle JP, Grigg ME, Arrizabalaga G, Boothroyd JC. Bioluminescence imaging of Toxoplasma gondii infection in living mice reveals dramatic differences between strains. *Infect Immun* 2005;**73**:695–702.

27. Di Pompo G, Salerno M, Rotili D, Valente S, Zwergel C, Avnet S, et al. Novel histone deacetylase inhibitors induce growth arrest, apoptosis, and differentiation in sarcoma cancer stem cells. *J Med Chem* 2015;**58**:4073–9.

28. Ramakrishnan C, Maier S, Walker RA, Rehrauer H, Joekel DE, Winiger RR, et al. An experimental genetically attenuated live vaccine to prevent transmission of Toxoplasma gondii by cats. *Sci Rep* 2019;**9**:1474.

29. Farhat DC, Swale C, Dard C, Cannella D, Ortet P, Barakat M, et al. A MORC-driven transcriptional switch controls Toxoplasma developmental trajectories and sexual commitment. *Nat Microbiol* 2020;**5**:570–83.

30. Hakimi M-A, Deitsch KW. Epigenetics in Apicomplexa: control of gene expression during cell cycle progression, differentiation and antigenic variation. *Curr Opin Microbiol* 2007;**10**:357–62.

31. Gissot M, Choi SW, Thompson RF, Greally JM, Kim K. Toxoplasma gondii and Cryptosporidium parvum lack detectable DNA cytosine methylation. *Eukaryot Cell* 2008 Epub ahead of publication 4 January 2008.

32. Farhat DC, Bowler M, Communie G, Pontier D, Belmudes L, Mas C, et al. A plant-like mechanism coupling m6A reading to polyadenylation safeguards transcriptome integrity and developmental genes partitioning in Toxoplasma. *bioRxiv* 2021;10.1101/2021.02.23.432502.

33. Holmes MJ, Padgett LR, Bastos MS, Sullivan WJ. m6A RNA methylation facilitates pre-mRNA 3'-end formation and is essential for viability of Toxoplasma gondii. *bioRxiv* 2021;10.1101/2021.01.29.428772.

34. Hammam E, Ananda G, Sinha A, Scheidig-Benatar C, Bohec M, Preiser PR, et al. Discovery of a new predominant cytosine DNA modification that is linked to gene expression in malaria parasites. *Nucleic Acids Res* 2020;**48**:184–99.

35. Martynowicz J, Doggett JS, Sullivan WJ. Efficacy of Guanabenz Combination Therapy against Chronic Toxoplasmosis across Multiple Mouse Strains. *Antimicrob Agents Chemother* 2020;**64**.

36. Doggett JS, Schultz T, Miller AJ, Bruzual I, Pou S, Winter R, et al. Orally Bioavailable Endochin-Like Quinolone Carbonate Ester Prodrug Reduces Toxoplasma gondii Brain Cysts. *Antimicrob Agents Chemother* 2020;**64**.

37. Mouveaux T, Roger E, Gueye A, Eysert F, Huot L, Grenier-Boley B, et al. Primary brain cell infection by Toxoplasma gondii reveals the extent and dynamics of parasite differentiation and its impact on neuron biology. *Open Biol* 2021;**11**:210053.

38. Ramakrishnan C, Walker RA, Eichenberger RM, Hehl AB, Smith NC. The merozoite-specific protein, TgGRA11B, identified as a component of the Toxoplasma gondii parasitophorous vacuole in a tachyzoite expression model. *Int J Parasitol* 2017;**47**: 597–600.

39. Alvarez CA, Suvorova ES. Checkpoints of apicomplexan cell division identified in Toxoplasma gondii. *PLoS Pathog* 2017;**13**:e1006483.

Table 1. Name, structure and potential target of the compounds tested.

Compounds	Molecular Structure	Potential target
MC1742	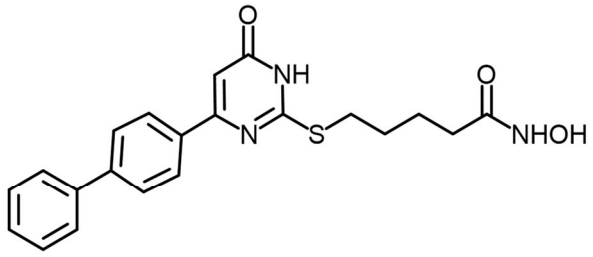	Histone Deacetylase (class I/IIb HDAC)
MC3973	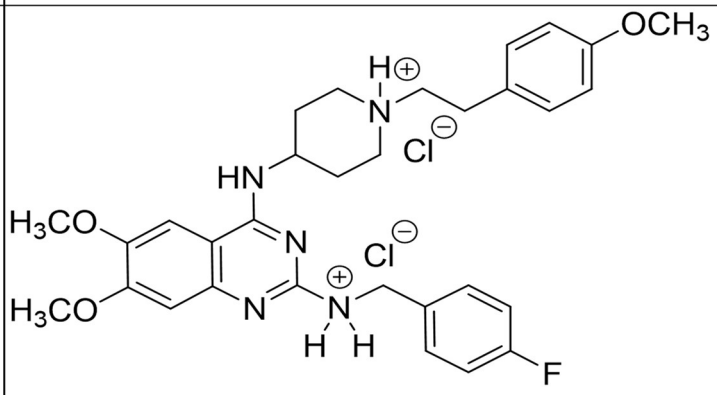	DNA methyl-transferase
MC3681	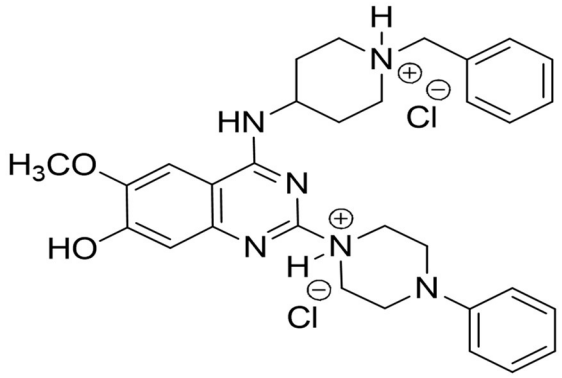	DNA methyl-transferase
Mocetinostat	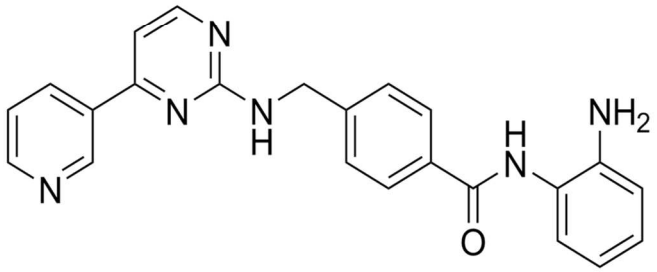	Histone Deacetylase (HDAC)

Table 2. IC_{50} of the compounds in Type I and Type II strains.

The IC_{50} on each *Toxoplasmosis gondii* strain was determined in at least three independent experiments. (1) IC_{50} in human fibroblasts (HFF cells) was determined in [21]. (2) Selectivity index was calculated based on the IC_{50} of the Type II strain.

	MC1742	**MC3681**	**MC3973**	**Mocetinostat**
Type I IC_{50} (nM)	34 ± 3	1447 ± 992	552 ± 390	365 ± 101
Type II IC_{50} (nM)	30 ± 8	1786 ± 904	512 ± 93	472 ± 270
HFF IC_{50} (nM)	3295 ± 247 (1)	7210 ± 14 (1)	3215 ± 389 (1)	ND
Selectivity index (2)	109	4	6	ND

Table 3. IC_{50} of selected hydroxamate-based compounds, apicidin and pyrimethamine.

Compounds	Structures	IC50 (nM)
MC1742	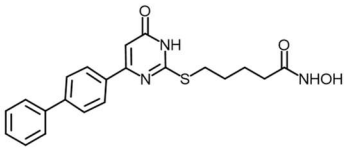	**30 ± 8 nM**
Pyrimethamine	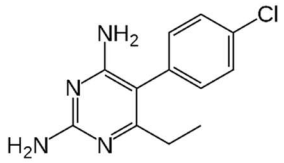	**660 ± 230 nM**
Trichostatin A	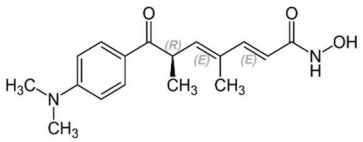	**176 ± 16 nM**
Scriptaid	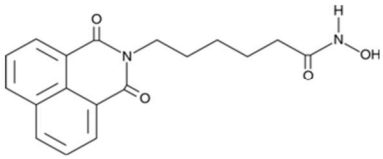	**316 ± 143 nM**
SAHA	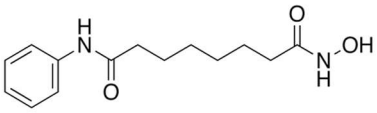	**247 ± 137 nM**
APICIDIN	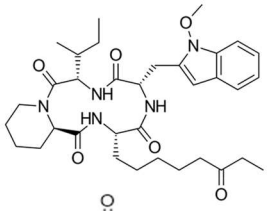	**14 ± 2 nM**
MC1714	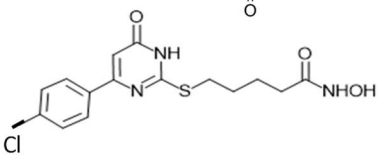	**748 ± 220 nM**
MC1745	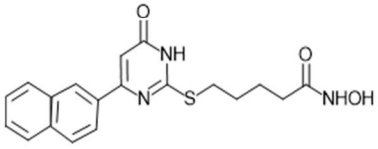	**374 ± 20 nM**
MC2026	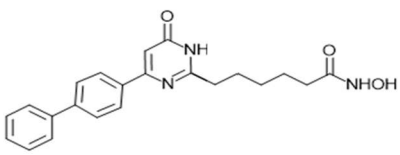	**501 ± 166 nM**

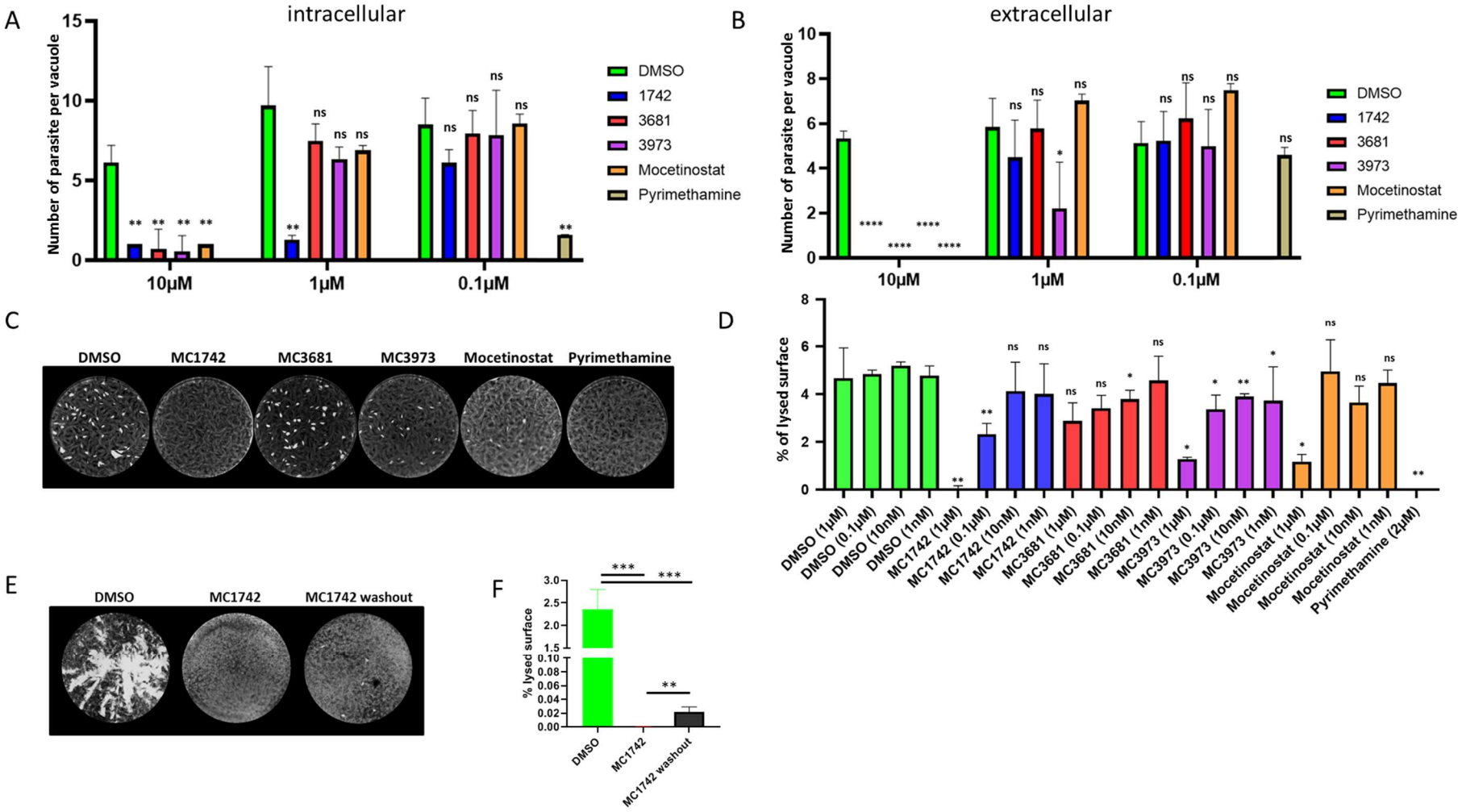

Figure 1. Compounds potentially active against epigenetic enzymes inhibit tachyzoite growth. (A) Effect of intracellular treatment of tachyzoites on intracellular growth. Tachyzoite intracellular growth was measured after 24 hours of exposure to different compounds at different concentrations

(10, 1 and 0,1 µM). The average number of parasites per vacuole was used as a metric of parasite intracellular growth. Parasites treated with DMSO (green bars) were used as a control. The effect of MC1742 (blue bars), MC3681 (red bars), MC3973 (pink bars), Mocetinostat (orange bars) and Pyrimethamine (brown bar, 2 µM) on intracellular growth was measured. The concentrations used for each drug are indicated on the x-axis. A Student's *t* test was performed with the DMSO as control; two-tailed *P*-value; ns: $P > 0.05$; *$P < 0.05$; **$P < 0.01$; mean ± sd (n = 3 independent experiments). **(B)** Effect of extracellular treatment of tachyzoites on intracellular growth. Tachyzoites intracellular growth was measured after 4 hours of extracellular exposure to different compounds at different concentrations (10, 1 and 0,1 µM). The average number of parasites per vacuole was used as a metric of parasite intracellular growth. Parasites treated by DMSO (green bars) were used as a control. The effect of MC1742 (blue bars), MC3681 (red bars), MC3973 (pink bars), Mocetinostat (orange bars) and Pyrimethamine (brown bar, 2 µM) on intracellular growth was measured. The concentrations used for each drug are indicated on the x-axis. A Student's *t* test was performed with the DMSO as control; two-tailed *P*-value; ns: $P > 0.05$; *$P < 0.05$; ****$P < 0.0001$; mean ± sd (n = 3 independent experiments). **(C)** Representative pictures of plaque assays after exposure to 1 µM of the compound. The name of the compound is indicated at top of each picture. **(D)** Quantification of the percentage of lysed surface on plaque assays. Plaque formation was observed after 7 days of exposure to different compounds at different concentrations (1, 0.1 and 0,01 µM). The percentage of lysed surface on the plaque assay was used as a metric of parasite growth and invasion ability. Parasites treated by DMSO (green bars) were used as a control. The effect of MC1742 (blue bars), MC3681 (red bars), MC3973 (pink bars), Mocetinostat (orange bars), and Pyrimethamine (brown bar, 2 µM) on plaque formation was measured. The name of the compound and concentrations used for each drug are indicated on the x-axis. A Student's *t* test was performed with the DMSO as control; two-tailed *P*-value; ns: $P > 0.05$; *$P < 0.05$; **$P < 0.01$; mean ± sd (n = 3 independent experiments). **(E)** Representative pictures of plaque assays after exposure to DMSO, 1 µM of MC1742 or 1 µM of MC1742 for 2 days and washout. **(F)** Quantification of the percentage of lysed surface on plaque assays. Parasites treated by DMSO (green bars) were used as a control. The effect of MC1742 continuous exposure (blue bars) after 8 days, or a washout experiment when parasites where exposed to MC1742 (1 µM) for 2 days and then the compound was washed-out and replaced by fresh media for 6 days (black bar, 2 µM) was measured on plaque formation. A Student's *t* test was performed with the DMSO as control; two-tailed *P*-value; ***$P < 0.001$; **$P < 0.01$; mean ± sd (n = 3 independent experiments).

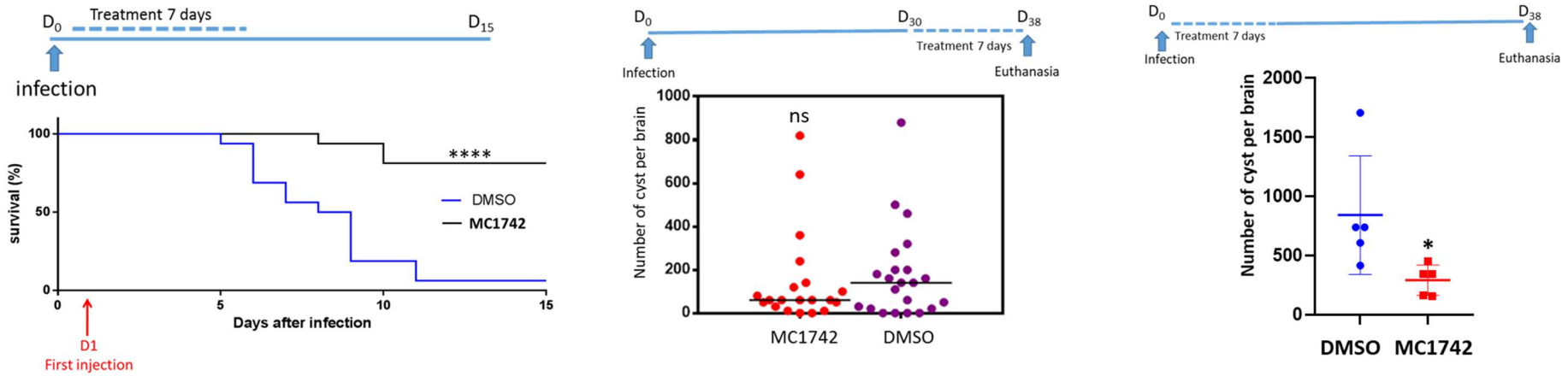

Figure 2

Figure 2. Effect of MC1742 on the outcome of the acute and latent toxoplasmosis. (A) Effect of MC1742 treatment on the outcome of acute disease. Tachyzoites were injected intraperitoneally and mice were treated 24 hours after infection with 10 mg/kg MC1742 once a day for 7 days. The percentage of mice surviving the lethal dose of Type II tachyzoites is represented for each day during 15 days. Mice treated with DMSO (same regimen, blue line) were used as a control. The percentage of surviving mice after treatment with MC1742 is indicated by a black line. A schematic representation of the experiment is indicated at the top of the figure. A Log-rank (Mantel-Cox) test was performed; ****$P < 0.0001$; mean ± sd (n = 32 mice per group). **(B)** Effect of MC1742 treatment on the latent form of the parasite. Tachyzoites were injected intraperitoneally and mice were left for 4 weeks. Mice were then treated with 10 mg/kg MC1742 once a day for 7 days. A schematic representation of the experiment is indicated at the top of the figure. The number of cysts per brain is represented for each mouse. Mice treated with DMSO (same regimen, purple dots) were used as a control. The number of cysts per brain after treatment with MC1742 is indicated by red dots. A Student's *t* test was performed; two-tailed *P*-value; ns: $P > 0.05$ (n = 20 mice per group). **(C)** Effect of MC1742 treatment on the establishment of the latent form of the parasite. Tachyzoites were injected intraperitoneally and mice were treated 24 hours after infection with 10 mg/kg MC1742 once a day for 7 days. Four weeks after the

end of the treatment, the brain cyst number for each individual was counted. A schematic representation of the experiment is indicated at the top of the figure. The number of cysts per brain is represented for each mouse. Mice treated with DMSO (same regimen, purple dots) were used as a control. The number of cysts per brain after treatment with MC1742 is indicated by red dots. A Student's *t* test was performed; two-tailed *P*-value; $*P < 0.05$ (n = 5 mice per group).

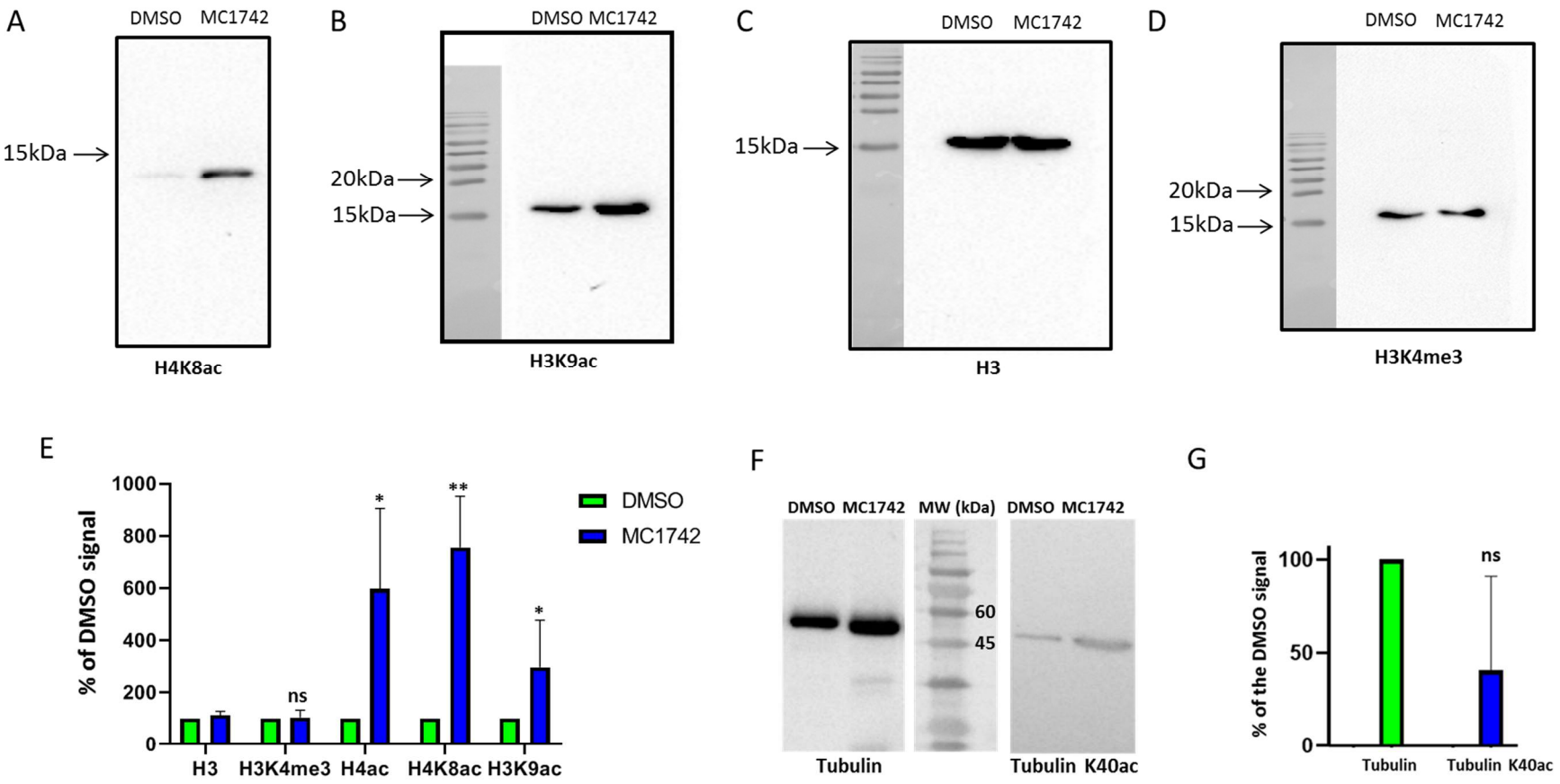

Figure 3

Figure 3. Hyper-actylation of *Toxoplasmosis gondii* histones after treatment with MC1742.

The purified parasite samples were either treated with DMSO or MC1742, as indicated at the top of each western blot. The molecular weight marker is indicated on the left side of the figure. The specific antibody used to reveal the relative abundance of the targeted histones is indicated at the bottom of the figure. **(A)** Western blot analysis of the acetylated histone H4 at the Lysine 8 residue. **(B)** Western blot analysis of the acetylated histone H3 at the Lysine 9 residue. **(C)** Western blot analysis of the histone H3 (modified and unmodified; antibody targeting the C-terminus of Histone H3) was used as an internal loading control. **(D)** Western blot analysis of the trimethylated histone H3 at the Lysine 4 residue. **(E)** Quantification of the signal for each indicated modified histone after treatment with DMSO (green bars) or MC1742 (blue bars). The signal was normalised to the signal given by the loading control (histone H3, modified and unmodified). A Student's *t* test was performed; two-tailed *P*-value; ns: $P > 0.05$; *$P < 0.05$; **$P < 0.01$; mean ± sd (n = 3 independent experiments). **(F)** Western blot analysis of the unmodified alpha tubulin and acetylated tubulin at the lysine 40. The molecular weight marker sizes are indicated. **(G)** Quantification of the signal for the acetylated tubulin normalised to the level of unmodified tubulin after treatment with DMSO (green bars) or MC1742 (blue bars). A Student's *t* test was performed; two-tailed *P*-value; ns: $P > 0.05$; mean ± sd (n = 3 independent experiments).

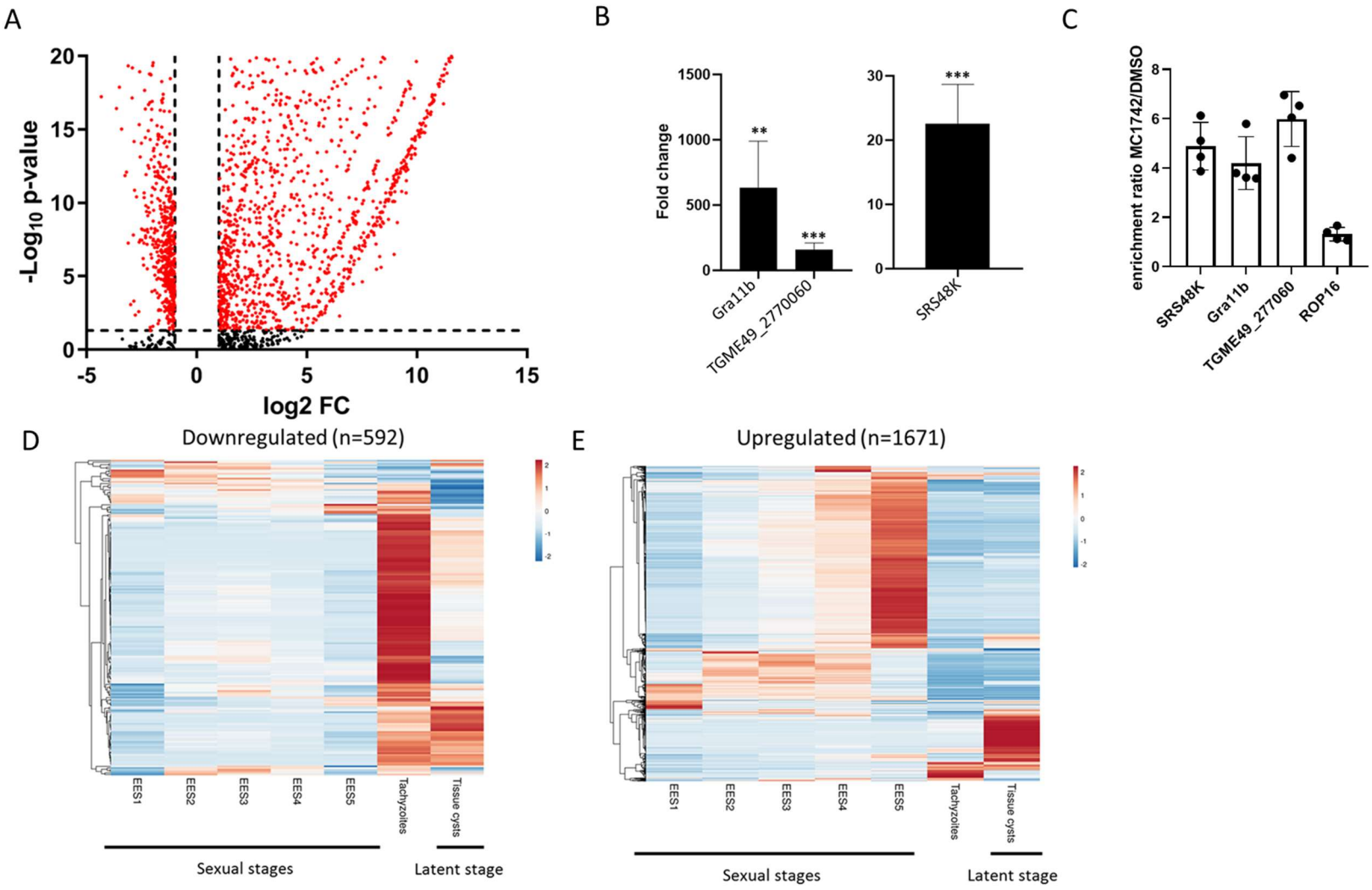

Figure 4. RNA-seq reveals the profound transcriptome changes after MC1742 treatment.

Samples were prepared by treating intracellular parasites (24 hours of growth) for 6 hours with DMSO or MC1742. **(A)** Volcano plot representing the distribution of the differentially expressed genes depending on their Log_2 fold change (log_2 FC, x-axis) and the associated $-Log_{10}$ *P*-value (y-axis). The horizontal dashed line represents the *P*-value cut-off (0.05) and the two vertical dashed lines represent the Log_2 fold change cut-off (1 or –1). Black dots represent genes that did not meet the *P*-value cut-off. Red dots represent the genes that met both cut-offs. For clarity, genes that did not meet the Log_2 fold change cut-off are not represented. The differential expression analysis was based on three independent biological experiments. **(B)** Verification by RT-qPCR of the expression of three genes that are upregulated after treatment by MC1742. The Log_2 fold change measured by RT-qPCR is represented. A Student's *t* test was performed with the DMSO as control; two-tailed *P*-value; $^{**}P < 0.01$; $^{***}P < 0.001$; mean ± sd (n = 3 independent experiments). **(C)** Verification by ChIP and qPCR of the enrichment of H4ac at the promoter of three genes that are upregulated after treatment by MC1742 (SRS48K, Gra11b, TGME49_277060) and a control locus (ROP16 promoter). The relative enrichment of H4ac at the tested promoter is represented as a ratio of the signal given by the MC1742 treated sample to the DMSO treated sample. **(D)** Heat map showing the expression during the *T. gondii* life cycle of all individual transcripts that are downregulated (n = 592) in the presence MC1742. The different sexual (EES1 to ESS5) and asexual (tachyzoites and tissue cysts) stages are indicated at the bottom of the figure. Data extracted from ToxoDB (www.toxodb.org) that was originally produced by Ramakrishnan et al. [28]. **(E)** Heat map showing the expression during the *T. gondii* life cycle of all individual transcripts that were upregulated (n = 1671) in the presence MC1742. The different sexual (EES1 to ESS5) and asexual (tachyzoites and tissue cysts) stages are indicated at the bottom of the figure. Data extracted from ToxoDB (www.toxodb.org) that was originally produced by Ramakrishnan et al. [28].

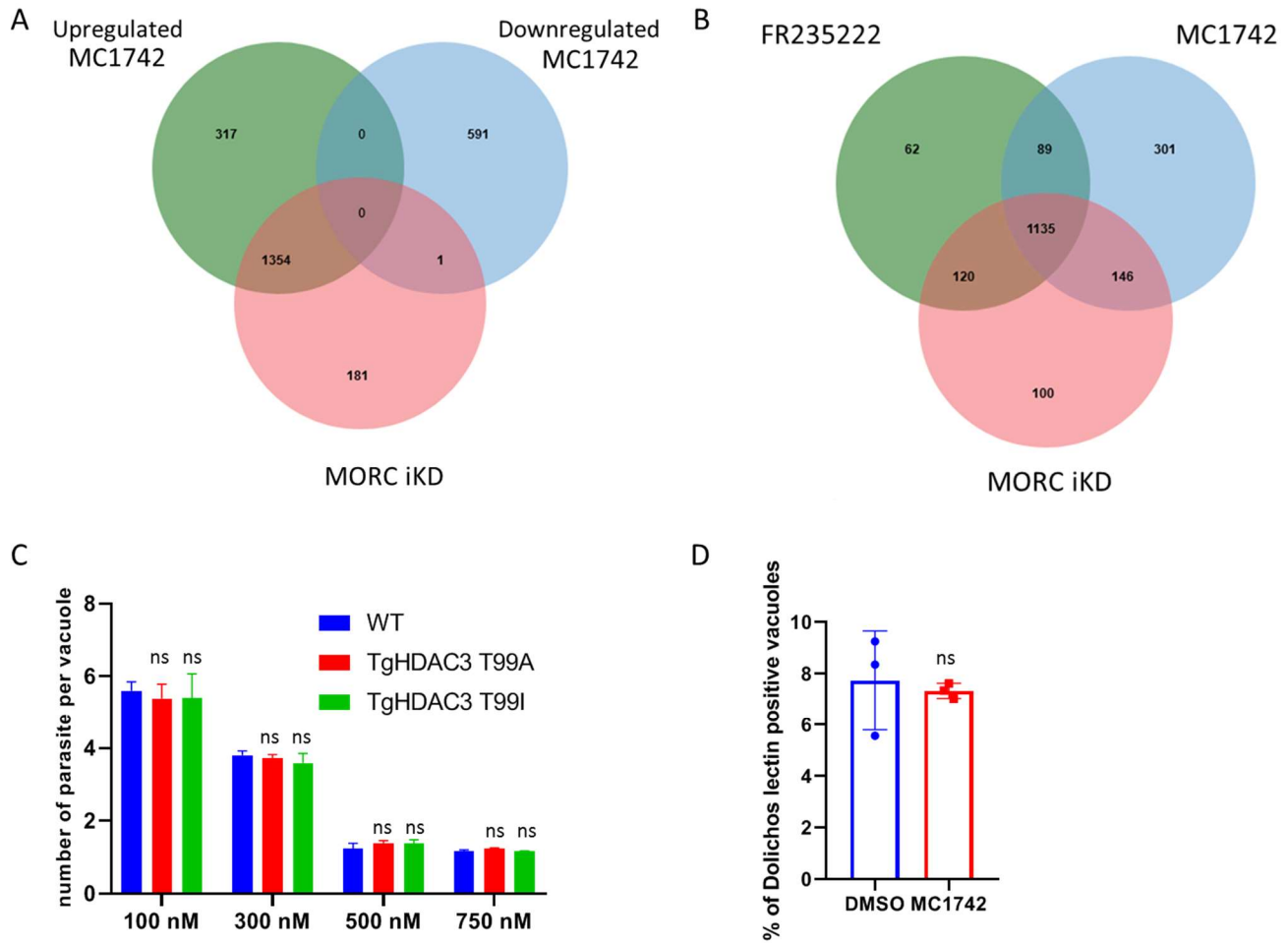

Figure 5. RNA-seq showed that MC1742 potential target may be TgHDAC3.

The list of differentially expressed genes was extracted from [29] and compared with the list of differentially expressed genes from the dataset. **(A)** Comparison of the differentially expressed genes that were upregulated (green circle) or downregulated (blue circle) after exposure to MC1742.

The upregulated genes after TgMORC knock-down (red circle) are represented in this Venn diagram. **(B)** Comparison of the differentially expressed genes that were upregulated (green circle) after FR235222 treatment (a specific inhibitor of TgHDAC3), upregulated after MC1742 treatment (blue circle) and the upregulated genes after TgMORC knock-down (red circle) showing a large overlap between these three datasets. **(C)** Tachyzoite intracellular growth was measured after 24 hours of exposure to MC1742 at different concentrations for the WT and FR235222-resistant strains bearing a mutation on TgHDAC3 (T99A or T99I). The average number of parasites per vacuole was used as a metric of parasite intracellular growth. The effect of MC1742 on the WT (blue bars), TgHDAC3 T99A (red bars) and TgHDAC3 T99I (green bars) strains was measured. The MC1742 concentrations (nM) used are indicated on the x-axis. A Student's *t* test was performed with the DMSO as control; two-tailed *P*-value; ns: $P > 0.05$; mean ± sd (n = 2 independent experiments). (D) Percentage of vacuoles labelled with *Dolichos biflorus* agglutinin (DBA). Tachyzoites of a type II strain were grown for 24 hours in the presence of 0.5 µM MC1742 and the number of vacuoles positive for DBA labelling was counted. A Student's *t* test was performed with the DMSO as control; two-tailed *P*-value; ns: $P > 0.05$; mean ± sd (n = 3 independent experiments).